JOURNAL OF CATALYSIS 140, 243–261 (1993)

# The Chain Mechanism in Catalytic Cracking

## The Kinetics of 2-Methylpentane Cracking

YINGXIAN ZHAO, G. R. BAMWENDA, W. A. GROTEN, AND B. W. WOJCIECHOWSKI[1]

*Department of Chemical Engineering, Queen's University, Kingston, Ontario, Canada K7L 3N6*

Received February 5, 1992; revised September 22, 1992

The cracking of 2-methylpentane on USHY at 300, 400, 450, and 500°C is interpreted in detail in terms of a chain mechanism. The kinetic equation developed from this mechanism fits the experimental data very well. The contribution of chain processes to the overall rate of conversion depends on the kinetic chain length, which in turn depends on the surface coverage by carbenium ions and their reactivities. Kinetic parameters were obtained at all four temperatures. A detailed examination of the kinetics shows that chain processes are more important at low reaction temperatures, whereas protolytic cracking dominates at higher temperatures. The parameters also show that both competitive inhibition by products and the rate of catalyst decay increase with increasing reaction temperature. Furthermore, they show that carbenium ions formed on Brønsted sites are more stable than carbonium ions. 

## INTRODUCTION

The mechanism of paraffin cracking on solid acids has been studied for many years and is still under debate (*2–14*). One issue concerns the initiation of the reaction. Although it is generally accepted that hydrocarbon cracking always involves ionic intermediates, there are various ideas concerning the formation of the carbenium ion. Hattori *et al.* (*15*) proposed that an abstraction of a hydride from the paraffin molecule by a Lewis acid site leads to the formation of an initial carbenium ion. Kramer *et al.* (*5*) suggested that paraffin molecules react with electron acceptor sites (*16*) to form radical ions which decompose to form smaller alkanes or hydrogen and olefins. Subsequently the olefins form carbenium ions on Brønsted acid sites. Weisz (*17*) proposed that the protonation of an olefin generated by thermal cracking, or present as an impurity in the feed, results in the formation of an initial carbenium ion on Brønsted sites. Haag and Dessau (*3*) as well as Corma *et al.* (*6*) propose that the initial carbenium ions result from the direct protonation of a feed paraffin by a Brønsted site to form a nonclassical pentacoordinated carbonium ion which decomposes to a carbenium ion and a small alkane or hydrogen. Recently, Lombardo and Hall (*8, 9*) studied the reaction of neopentane and isobutane over zeolite catalysts with varying acid strength. They too propose that the reaction is initiated via the direct protolysis of C–C or C–H bond in the feed molecule to form an alkane or hydrogen and a carbenium ion. Their data shows that in the case of isobutane, both C–C and C–H bond cleavage takes place, while in the case of neopentane, only protolysis of the C–C bond occurs, suggesting that primary hydrogens are difficult to protolyze. Once the initial carbenium ion is formed, most authors agree that it can undergo desorption, isomerization, $\beta$-scission, etc. There is also a consensus that the carbenium ions must take part in other reactions, but the processes by which they do this were never quantified.

A second topic we address is the process

[1] To whom correspondence should be addressed.



0021-9517/93 $5.00

of isomerization of paraffins. Pikert *et al.* (*18*) and Tung and McIninch (*19*), for example, have suggested that the cracking and isomerization of a paraffin take place via two independent, parallel pathways. We will try to show that all the observations available are also explained if we assume that isomerization takes place via the rearrangement of a carbenium ion containing the same number of carbons as the feed molecule (a "parent" ion) followed by a hydride transfer from a feed molecule to the isomerized parent ion in a process which is intimately connected to the other events occuring in catalytic cracking. The question is therefore: how is the parent carbenium ion formed, since the initial product does not contain the same number of moles of molecular hydrogen as there are of isomerized feed?

The kinetics of paraffin cracking have previously been studied in various systems in our laboratory (*1*, *20–22*). Abbot and Wojciechowski developed and presented a "monomolecular" reaction model which describes the cracking rates of all linear paraffin molecules studied to date (*20*). This model was recently extended by Groten and Wojciechowski to include a "bimolecular" or "chain" component of reaction (*1*). This latest formulation fits all the hydrocarbon cracking rate data we have gathered to date, including that for all linear alkanes which were found to obey the simplified form of the more general model of Groten and Wojciechowski (*1*), as presented by Abbot and Wojciechowski (*20*). In all the linear alkane cracking reactions the kinetic equation did not require the term accounting for chain processes in order to fit the data.

In the present work, 2-methylpentane was cracked on HY zeolite at temperatures ranging from 300 to 500°C. A discussion of the details of the mechanism and kinetics is presented below, and we show that for this case the second-order ("chain") term is necessary at all temperatures to fit the conversion data adequately. We take this to indicate that this molecule cracks in large part via chain processes.

*Assumptions and Definitions*

A systematic methodology for determining the selectivity of products has been previously reported (*23*, *24*). For each reaction product, the time-averaged yield sampled from $t = 0$ to $t_f$ is plotted against the time-averaged conversion. Each such plot can be enveloped by a single curve, the optimum performance envelope (OPE), which describes the selectivity behaviour of that product as catalyst age approaches zero. A product is considered primary if the slope at the origin of such a curve is nonzero and secondary if the slope is zero. Primary products are those which are formed directly from the feed molecule without any detectable gas-phase intermediate. We use this identification of primary products to guide our discussion of the reaction mechanism.

In order to quantify the processes for the formation of the primary products, we make certain assumptions regarding the behavior of their precursor ions on the catalyst surface. It is impossible to measure the concentrations of these surface species directly, however, we can safely assume that their amounts are much smaller than those of reactant or products. We also assume that these surface species rapidly establish an equilibrium with the corresponding gas phase olefins. This approximation gives a correct and easily developed form of the rate expression, but may distort the significance of some of the parameters. A more rigorous solution requires that surface species concentrations be calculated using a steady-state assumption. This approach gives the same form of the final rate equation, but assigns a somewhat different meaning to some of the parameters which appear in the rate expression. Thus we say that

$$r_i = \frac{d[P_iS]}{dt} = 0, \qquad (1)$$

where $r_i$ is the net rate of change of the $i$th surface species concentration. Furthermore, since we assume that product olefins are in equilibrium with their carbenium ions (not at steady state),

$$[P_iS] = K_{p_i}[P_i][S], \qquad (2)$$

where $[P_iS]$ is the $i$th surface ion concentration, $[P_i]$ is the $i$th olefin product concentration, $[S]$ is the active site concentration, and $K_{p_i}$ is the $i$th product adsorption constant.

Finally, the time-on-stream theory of catalyst decay (*24, 25*) states that the active site concentration is a function of time on stream,

$$[S] = [S_0](1 + Gt)^{-M}, \qquad (3)$$

where $[S_0]$ is the initial concentration of active sites, $G$ is the aging parameter, $M$ is the aging exponent, and $t$ is catalyst time-on-stream.

These concepts serve as a basis for formulating the rate expression describing the chain mechanism of catalytic cracking. In order to apply these ideas, we first obtained data on the catalytic cracking of 2-methylpentane at 400°C over USHY to serve as our model system, and then expanded the investigation using a different apparatus (and a different operator) at 300, 400, 450, and 500°C.

## EXPERIMENTAL

The feedstock, 2-methylpentane of 99+% purity, was obtained from Aldich and used without further purification. The major impurities were 3-methylpentane and 2,3-dimethylbutane.

USHY zeolite was prepared from NaY (BDH CHEM., Lot. No. 45912, 13Y) according to the methods described in the literature (*26*). After steaming for 24 h at 473 K and 1 atm, the powder was compressed into pellets and crushed. Catalyst particles with mesh size 80/100 were used in all experiments.

Reaction runs were carried out in a fixed-bed, gas-phase, plug-flow reactor with an independently controlled three zone heater. The catalyst bed (0.15 m long) consists of catalyst diluted by silica of the same mesh size in order to minimize the thermal effects of reaction. Details of the experimental apparatus and of the methodology have been reported previously (*27*). Blank runs were carried out to determine the extent of thermal cracking.

Products were identified by the use of a Finnigan 1020 automated GC/MS. The gaseous products were analyzed using a Carle SX 1156 gas chromatograph which enables the direct determination of hydrogen. The liquid products were analyzed using a Varian 3700 gas chromatograph with an SE54 capillary column and a flame ionization detector. Products up to $C_7$ were eluted at 15°C followed by a temperature ramp of 5°C/min up to 300°C.

After each run the reactor was purged with dry $N_2$ for 20 min. All unpurged residues were regarded as coke. To quantify the amount of coke deposited during a run, carbon dioxide-free air was passed through the catalyst at 500°C. The water formed was collected in two drierite tubes in series and the carbon dioxide in two ascarite tubes. Complete combustion to carbon dioxide was assured by passing the dried combustion stream through a reactor containing a combustion catalyst. The hydrogen and carbon contents of the coke were calculated from the collected weight of water and carbon dioxide.

## RESULTS AND DISCUSSION

### *Initiation Reaction*

Some examples of the OPEs of products from 2-methylpentane cracking at 400°C are presented in Fig. 1. Table 1 shows the values of all initial selectivities determined at 400°C from such curves. We see that initial products consist of paraffins in the range $C_1$–$C_6$, olefins in the range of $C_2$–$C_6$, hydrogen and coke.

The classical $\beta$-scission into two fragments must always result in a product par-

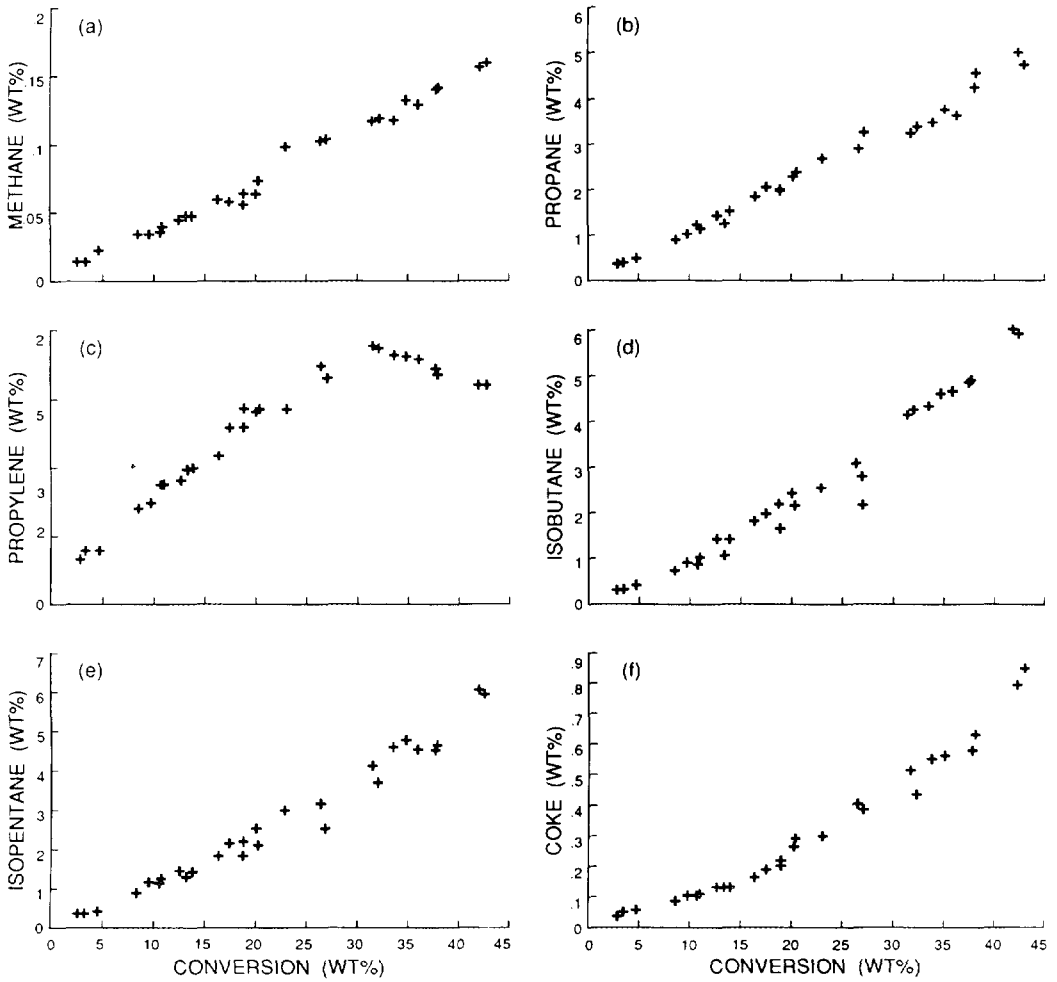


FIG. 1. Optimum performance envelopes for products from 2-methylpentane cracking at 400°C: (a) methane, (b) propane, (c) propylene, (d) isobutane, (e) isopentane, and (f) coke.

affin to olefin molar selectivity ratio of one or less. Data in Table 2 clearly shows that 2-methylpentane cracking on USHY does not obey this simple pattern in many details. For example, the presence of $C_6$ olefins in the initial product in total amount greater than that of the initial molecular hydrogen cannot be explained by any conventional mechanism. To account for this and other observations we propose that the product yields are complicated due to the presence of chain processes.

*Monomolecular and Bimolecular Processes*

Most workers will agree that following the protolysis of a feed molecule by the initiation reaction, the residual carbenium ion can undergo desorption as an olefin or $\beta$-scission to produce an olefin and a smaller residual carbenium ion. Obviously, the paraffin/olefin molar selectivity ratio in products which result from this process must always be $\leq 1$. Such a monomolecular

TABLE 1

Initial Selectivities for Reaction of 2-Methylpentane on HY at 400°C

| Product | Initial selectivity | | | |
|---|---|---|---|---|
| | Weight | Molar | | |
| | | Molecule | C | H |
| Hydrogen | 0.0004 | 0.0172 | — | 0.0344 |
| Methane | 0.0030 | 0.0161 | 0.0161 | 0.0644 |
| Ethane | 0.0021 | 0.0060 | 0.0120 | 0.0360 |
| Ethylene | 0.0066 | 0.0203 | 0.0406 | 0.0812 |
| Propane | 0.0955 | 0.1867 | 0.5601 | 1.4936 |
| Propylene | 0.0976 | 0.1999 | 0.5997 | 1.1994 |
| Isobutane | 0.0595 | 0.0882 | 0.3528 | 0.8820 |
| *n*-Butane | 0.0229 | 0.0340 | 0.1388 | 0.3470 |
| C4 olefins | 0.0117 | 0.0180 | 0.0720 | 0.1440 |
| Isopentane | 0.0814 | 0.0973 | 0.4865 | 1.1676 |
| *n*-Pentane | 0.0069 | 0.0082 | 0.0410 | 0.0984 |
| C5 olefins | 0.0065 | 0.0080 | 0.0400 | 0.0800 |
| 2,3-DMButane | 0.0853 | 0.0853 | 0.5118 | 1.1942 |
| 3-Methylpentane | 0.4151 | 0.4151 | 2.4906 | 5.8114 |
| *n*-Hexane | 0.0472 | 0.0472 | 0.2832 | 0.6608 |
| C6 olefins | 0.0487 | 0.0498 | 0.2991 | 0.5982 |
| Coke | 0.0086 | 0.0101 | 0.0528 | 0.1031 |
| Totals | 0.9990 | 1.3074 | 5.9971 | 13.9957 |

mechanism cannot explain the presence of initial $C_5$ paraffins, the $C_4$ paraffin to $C_2$ olefin ratio, or the $C_6$ olefin to $H_2$ ratio observed here.

We propose that even at low conversion (i.e., initial conditions) bimolecular processes take place between feed molecules and various carbenium ions, formed by the initiation processes and left on the catalyst surface. One such bimolecular process is "hydride transfer" leading to the formation of a gas-phase paraffin from the original carbenium ion, and a $C_6$ carbenium ion, formed from the feed. The other is "dimerization cracking" leading to the formation of a paraffin and a new carbenium ion which may be smaller or larger than the feed:

$$C_nH_{2n+1}S^+ + C_6H_{14} \rightarrow C_nH_{2n+2} + C_6H_{13}S^+ \quad (4)$$

$$C_nH_{2n+1}S^+ + C_6H_{14} \rightarrow C_{n+x}H_{2(n+x)+2} + C_{6-x}H_{13-2x}S^+. \quad (5)$$

We call such events "chain propagation" processes, implying that they may be repeated several times before a given site reverts to a Brønsted acid by the desorption of an olefin. They also constitute events which play the role of "hydrogen transfer reactions."

TABLE 2

Molar Selectivity of each Fragment in the Reaction of 2-Methylpentane on HY at 400°C

| Molar selectivity | | | | Ratio |
|---|---|---|---|---|
| Paraffin | | Partner olefin | | Paraffin/olefin |
| C1 | 0.0161 | C5 | 0.0080 | 2.013 |
| C2 | 0.0060 | C4 | 0.0180 | 0.333 |
| C3 | 0.1867 | C3 | 0.1999 | 0.934 |
| C4 | 0.1222 | C2 | 0.0203 | 6.054 |
| C5 | 0.1055 | | | |
| Total | 0.4365 | | 0.2462 | 1.7729 |
| H2 | 0.0172 | C6 | 0.0498 | 0.345 |
| C6 | 0.5476 | | | |

*Isomerization and Cracking*

There is also general agreement that carbenium ions can rearrange to form skeletal isomers, however, the desorption of such species from Brønsted sites will only produce isomeric olefins. It is more difficult to explain the mechanism producing paraffinic isomers of the feed molecule. There are three $C_6$ isomeric paraffins in our product (Table 1), with a molar selectivity ratio of 3-methylpentane/2,3-dimethylbutane/*n*-hexane of 0.415/0.085/0.047. We propose that this isomerization occurs via the chain mechanism involving a parent carbenium ion.

Although there is some evidence that isomerization of paraffins occurs on Lewis acid sites in the superacid systems $P_2O_5/Al_2O_3$ and $AlCl_3/Al_2O_3$ (*15, 28*) in our case, and in most studies of catalytic cracking, there is no evidence of activity of the pristine Lewis sites present on the inorganic catalyst framework and it seems more reasonable to think that all $C_6^+$ carbenium ions are associated with Brønsted sites. The appearance of $C_6$ olefins, which can only be

formed by the desorption of a $C_6^+$ carbenium ion from a Brønsted site, tends to support this view. Now, the parent $C_6^+$ carbenium ion may be formed by the direct protolysis of a C–H bond in the feed molecule in an initiation event or by a hydride transfer from a feed molecule to a surface carbenium ion in a chain propagation step. Once formed, the $C_6^+$ carbenium ion can undergo skeletal rearrangement and then abstract a $H^-$ from a subsequent feed molecule (Eq. (4)), to produce a $C_6$ isomeric paraffin product and a new $C_6^+$ carbenium ion. Such a process readily accounts for all the $C_6$ paraffin isomers found in the products. As to the ratio of the three $C_6$ isomeric paraffins, we agree with other workers (*29, 30*) that this reflects differences of stabilities in the structures of the corresponding carbenium ions.

According to the above discussion, the pathways for isomerization and cracking are not independent. They are alternative events in the conversion of feed by a chain reaction mechanism, which we discuss in more detail below.

*Paraffin-to-Olefin Ratio*

In order to explain the paraffin-to-olefin ratio we note that various previous studies (*20–22*) have shown that the "excess" hydrogen found in the "excess" paraffins of the gas phase does not result from any influx of hydrogen to the organic products of the reaction. The same is true here as shown in Table 1. We propose therefore that "excess" paraffins are formed by hydrogen transfer between feed molecules and surface carbenium ions. Such a process will result in the formation of a gas-phase paraffin and a new carbenium ion. Each repetition of such an event in the chain propagation process yields a paraffin product molecule, but no olefin. Further support for this mechanism comes from a detailed examination of the selectivity ratios, as we will show elsewhere.

Olefinic carbenium ions which arise by hydrogen abstraction from product olefins can be thought of as "precoke" in the sense that such species may not be entirely unreactive in chain processes, while at the same time they are more dehydrogenated than the average carbenium ion. By undergoing a subsequent hydrogen transfer from a gas-phase feed molecule, such a precoke species can also produce a gas-phase olefin and a new parent carbenium ion, thus making no difference to the paraffin/olefin ratio in the products. Depending on the reactivity of the various types of carbenium ions, including precoke, the total activity of the catalyst changes with time on stream as the population of surface species evolves in ways described by Rice and Wojciechowski (*31*). Carbenium ions can also evolve by undergoing thermal elimination of hydrogen, or of small paraffins, or by the surface disproportionation of two carbenium ions. These various processes lead to a small excess of paraffins, to a decrease in the activity of the average residual ion, hence to catalyst decay, and to a hardening of the coke. Coke-making processes will be discussed in detail elsewhere, the main point here being that the paraffin/olefin ratio is distorted by various bimolecular reactions involving carbenium ions.

## THEORY

*Kinetics*

We formulate the chain mechanism of catalytic cracking by writing the following elementary steps:

*1. Chain initiation.* The reaction is initiated by the protolysis of any C–C bond or of a C–H bond in the feed molecule

$$C_6H_{14} + SH \underset{k_0}{\overset{k_0}{\rightleftharpoons}} C_6H_{15}S^+ \xrightarrow{ak_{in}} C_nH_{2n+1}S + C_{6-n}H_{2(6-n)+2}, \quad n = 2,6 \quad (6)$$

where $C_6H_{14}$ is a feed molecule, SH is a Brønsted acid site, $C_nH_{2n+1}S^+$ is a carbenium ion associated with a Brønsted site, $C_{6-n}H_2(6-n)+2$ is a product paraffin, and $k$ is a rate constant of an elementary reaction.

*2. Chain transfer.* Larger ions can rearrange to form skeletal isomers

$$C_nH_{2n+1}S^+ \underset{{}_{in}k_n}{\overset{{}^{n}k_{in}}{\rightleftharpoons}} i - C_nH_{2n+1}S^+, \quad (7)$$

where $i - C_nH_{2n+1}S^+$ is a skeletal isomer of a carbenium ion with $n \geq 4$.

Alternatively, they can crack by $\beta$-scission

$$C_jH_{2j+1}S^+ \xrightarrow{{}^{j}k_{in}} C_nH_{2n+1}S^+ + C_{j-n}H_{2(j-n)}, \quad 6 \leq j \leq 6 + n. \quad (8)$$

*3. Chain propagation.* Chain propagation is carried out by bimolecular process between a carbenium ion and a feed molecule:

$$C_nH_{2n+1}S^+ + C_6H_{14} \xrightarrow{{}^{n}k_{2j}} C_jH_{2j+1}S^+ + C_{6+n-j}H_{2(6+n-j)+2}, \quad j \geq n. \quad (9)$$

The process in Eq. (9) may be repeated resulting in a number of chain events, depending on reaction conditions.

*4. Chain termination.* The reaction chain is terminated by the desorption of a carbenium ion to yield an olefin. The reverse process will also take place so that an equilibrium may exist:

$$C_nH_{2n+1}S + \underset{{}_{0}k_n}{\overset{{}^{n}k_0}{\rightleftharpoons}} C_nH_{2n} + SH, \quad 2 \leq n \leq 6 \quad (10)$$

Carbenium ions will also be involved in coke formation and activity decay as discussed above. The number of ions which take this route is very small and will be neglected in the following kinetic development.

Using the approximations of Eqs. (1) and (2) in the mechanism consisting of Eqs. (6), (7), (8), (9), and (10), we obtain the rate equation for the overall conversion in a plug flow reactor,

$$\frac{dX}{d\tau} = \left( \frac{A_1 \left( \frac{1 - X}{1 + \varepsilon X} \right) + A_2 \left( \frac{1 - X}{1 + \varepsilon X} \right)^2}{1 + B \left( \frac{1 - X}{1 + \varepsilon X} \right)} \right) \times [S]_0(1 + Gt)^{-N}, \quad (11a)$$

where $X$ is the fractional conversion of feed, $\tau$ is the space time, $\varepsilon$ is the volume expansion coefficient, $t$ is the time on stream, $[S]_0$ is the initial concentration of active sites, and $G$ and $N$ are aging parameters.

This is identical with the equation developed from a simplified model by Groten and Wojciechowski (*1*). Parameters $A_1$, $A_2$, and $B$ are here defined by the expressions

$$A_1 = \frac{(k_0I_1/I_0) + \sum_{n=2}^{6} \mathcal{F}_n \cdot I_n \cdot {}_nK_n[C_6H_{14}]_0}{1 + (\sum_{n=2}^{6} \mathcal{F}_n {}_nK_n + \sum_{n=4}^{6} \mathcal{F}_n {}_nK_n K_{nn})[C_6H_{14}]_0} \quad (12a)$$

$$A_2 = \frac{-\sum_{n=2}^{6} \mathcal{F}_n \cdot I_n \cdot {}_nK_n[C_6H_{14}]_0}{1 + (\sum_{n=2}^{6} \mathcal{F}_n {}_nK_n + \sum_{n=4}^{6} \mathcal{F}_n {}_nK_n K_{nn})[C_6H_{14}]_0} \quad (12b)$$

$$B = \frac{[k_0/I_0 - \sum_{n=2}^{6} \mathcal{F}_n \cdot {}_nK_n + \sum_{n=4}^{6} \mathcal{F}_n {}_nK_n K_{nn})[C_6H_{14}]_0}{1 + (\sum_{n=2}^{6} \mathcal{F}_n {}_nK_n + \sum_{n=4}^{6} \mathcal{F}_n {}_nK_n K_{nn})[C_6H_{14}]_0}, \quad (12c)$$

where $\mathcal{F}_n$ is the molar selectivity of product olefin $C_nH_{2n}$, $K_{nn}$ is the skeletal isomerization equilibrium constant for carbenium ion $C_nH_{2n+1}S^+$, ${}_nK_n$ is the adsorption equilibrium constant for product olefin $C_nH_{2n}$, and $[C_6H_{14}]_0$ is the initial concentration of the feed.

Integrating Eq. (11a) with respect to $\tau$ at constant $t$, with $\tau = 0$, $X = 0$ and using the relationship $\tau = bPt_f$, gives

$$\phi_1 \ln(\phi_2 + \phi_3 X) - \phi_4 \ln(1 - X) - \phi_5 X - \phi_6 - bPt_f[SH]_0(1 + Gt)^{-N} = 0, \quad (11b)$$

where $\phi_i$ are functions of the parameters $A_1$, $A_2$, $B$, and $G$, $P$ is the catalyst/reactant

weight ratio, $b$ is the reactant/catalyst density ratio, and $t_f$ is the total run time. A detailed development of Eqs. (11a) and (11b) is presented in Appendix A, Part I.

Figure 2 shows that our experimental data is well presented by Eq. (11). The optimum values of kinetic parameters $A_1$, $A_2$, $B$, and $G$ are presented in Table 3 together with a statistical measure of fit.

We note that $B = -0.902$ which requires that the second term of the denominator is larger than the first and suggests that

$$\left(\sum_{n=2}^{6} \mathcal{F}_n \cdot {}_nK_n + \sum_{n=4}^{6} \mathcal{F}_n \cdot {}_nK_n \cdot K_{nn}\right) [C_6H_{14}]_0 \gg 1; \quad (13a)$$

this leads to

$$B + 1 = \frac{k_0/I_0}{\sum_{n=2}^{6} \mathcal{F}_n \cdot {}_nK_n + \sum_{n=4}^{6} \mathcal{F}_n \cdot {}_nK_n \cdot K_{nn}}, \quad (13b)$$

and since $(B + 1) = 0.098$, the numerator is much smaller than the denominator. This parameter keeps the same form regardless of whether we use the equilibrium or the steady-state solution and therefore can be analyzed in more detail.

*Kinetic Chain Length*

We define KCL, the kinetic chain length, as

$$\text{KCL} = \frac{\text{Overall rate}}{\text{Rate of initiation}}. \quad (14)$$

This yields the expression (Appendix A, Part II)

$$\text{KCL} = 1 + \frac{\sum_{n=2}^{6} \mathcal{F}_n \cdot I_n \cdot {}_nK_n(1 + \epsilon)X/(1 + \epsilon X)}{k_0 \cdot I_i/I_0} [C_6H_{14}]_0. \quad (15)$$

Obviously, KCL is a function of olefin selectivity $\mathcal{F}_n$ and of the conversion $X$. Abbot and Wojciechowski (*12*) showed that on a catalyst only slightly different from that used here, curves of $\bar{X}_f$ vs TOS for a number of branched paraffins exhibit a sigmoidal shape (Fig. 3). Simulations of this effect are reported by Groten and Wojciechowski (*1*) and indicated that such an effect will arise when the reaction proceeds mainly via the chain mechanism, i.e., when the chain length is large. Since sigmoidality is not noticeable in Fig. 2, we conclude that chain length is very sensitive to catalyst preparation methods.

There is a second line of evidence for the existence of chain processes in circumstances so sensitive to the details of the experimental system under investigation, that a long-running debate has ensued. Much confusion has resulted from the contradic-

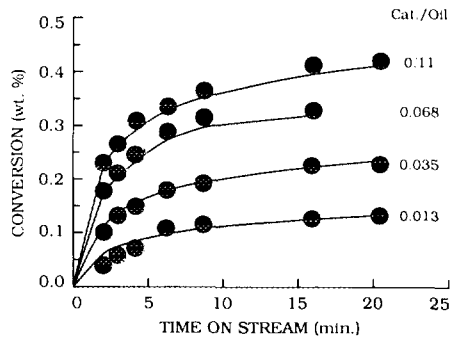


FIG. 2. Theoretical curves and experimental points for 2-methylpentane cracking on USHY at 400°C.

TABLE 3

Kinetic Parameters for the Reaction of 2-Methylpentane on HY at 400°C

| $A_1$ (min$^{-1}$) | $A_2$ (min$^{-1}$) | $B$ | $G$ (min$^{-1}$) | $N$ | $B + 1$ | $\frac{A_1 + A_2}{-A_2}$ |
|---|---|---|---|---|---|---|
| 0.278 | −0.0838 | −0.902 | 0.262 | 1 | 0.098 | 2.317 |

*Note.* Kinetic parameters $A_1$, $A_2$, $B$, $G$, and $N$ were obtained by fitting experimental conversion data using Eq. (11). All runs were carried out in a plug flow reactor at 1 atm.

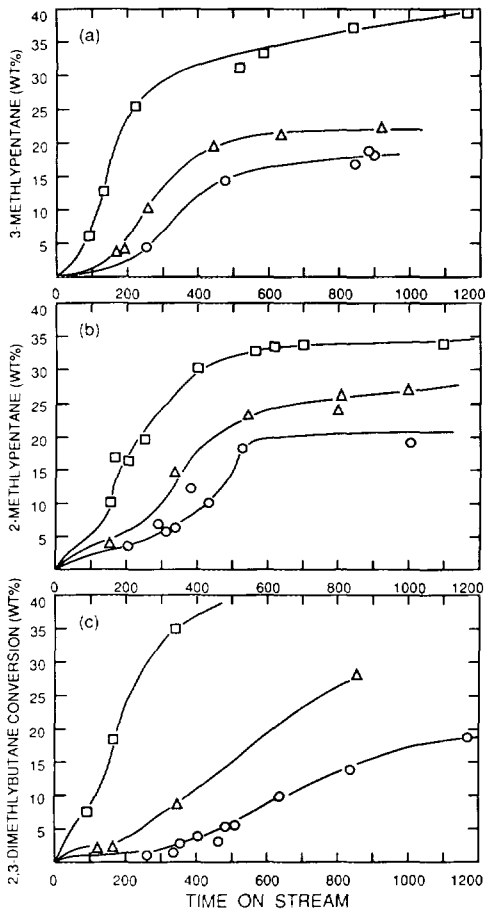


FIG. 3. Curves of $\bar{X}_f$ vs TOS for a number of branched $C_6$ paraffins cracking on HY at 500°C (*12*), catalyst-to-reactant weight ratios: (□) 0.0385, (△) 0.0154, and (○) 0.0077. (a) 3-methylpentane, (b) 2-methylpentane, and (c) 2,3-dimethylbutane.

tory evidence concerning the effects of added olefins on the overall rate of reaction. Figure 4 shows a sigmoidal curve of the kind reported by Abbot and Wojciechowski (*12*). The induction period at small values of $X$ occurs only if the concentration of product olefins is too small to make the acceleration due to the increasing contribution of chain processes to overall conversion significant. This in turn depends on the value of $A_2$ appropriate for that catalyst. Now, if we add an olefin to this system, we artificially produce a real and high value of at least one $\mathcal{F}_n$ and hence a higher value of $-A_2$, i.e., forcing a greater contribution from chain reactions, even at low conversions of the feed. The result is that the induction period is reduced as shown in Fig. 4. Since most such experiments were carried out at "standard conditions," an increased conversion was observed and an increased rate of reaction inferred. This phenomenon has proved to be ephemeral and the reasons for this are now clear. In order to observe the effect one should start with a catalyst which will propagate long chains. No other system will show acceleration by added olefin and catalysts prepared in very similar ways may show very different behaviours. Next, one must chose an olefin which is an effective chain propagator (large ${}_nk_{2n}$ in $I_n$ of Eq. (12b)). Last but not least one must add enough of this olefin to make $\alpha_n$ significant so that the parameter $A_2$ is made large. This seems to have happened in some studies (*2*, *32*, *33*) and not in others (*22*, *34*, *35*).

### *Temperature Effects in 2-Methylpentane Cracking*

*Thermal cracking.* Experiments performed using deactivated silica packing in place of the catalyst showed that detectable thermal cracking of 2-methylpentane occurs in the temperature range 400 to 500°C. Conversion due to thermal cracking varied with time on stream as shown in Fig. 5. Although thermal conversion was below

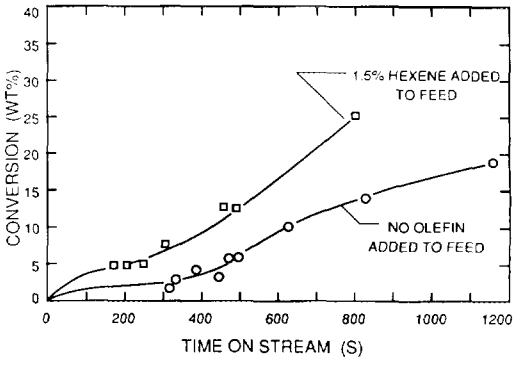


FIG. 4. The effect of added olefin on 2,3-dimethylbutane cracking on HY at 500°C (*12*).

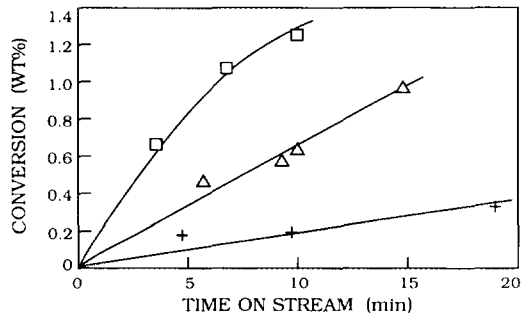


FIG. 5. Thermal conversion of 2-methylpentane on deactivated silica at various temperatures: (+) 400°C, (△) 450°C, and (□) 500°C.

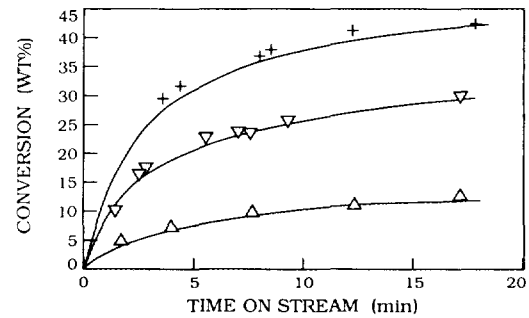


FIG. 7. Theoretical curves and experimental points for the reaction of 2-methylpentane on USHY at 400°C, catalyst-to-reactant ratios: (△) 0.0077, (▽) 0.043, and (+) 0.104.

2% at the severest conditions used at 500°C, it could influence the interpretation of catalytic cracking results. For this reason, the catalytic conversions used for model fitting were obtained by subtracting thermal from total conversion at the same time on stream.

*Catalytic cracking.* Figures 6 to 9 present experimental catalytic conversion points and the corresponding lines of calculated conversion as a function of time on stream for various constant catalyst to reactant ratios using our best fit parameters. These optimum values of the kinetic parameters were determined using the sum of squares of residuals as the criterion of fit and are reported in Table 4. The fit obtained was found to be satisfactory by the $F$-test at the 95% confidence level for all four temperatures, and the parameters obtained at 400°C in this set of experiments compare well with those obtained in an independent study and reported in Table 3. The value of the decay exponent $N$ was found to be close to one at all temperatures when allowed to vary and its value was fixed at 1.0 (*23*).

It should be noted that whereas the $A_2$ parameter was not necessary to fit $n$-nonane kinetics or for that matter the kinetics of cracking of any of the linear paraffins studied to date (*1*), it is necessary to obtain a satisfactory fit for 2-methylpentane, not only at 400°C as reported above, but at each temperature studied here. This suggests

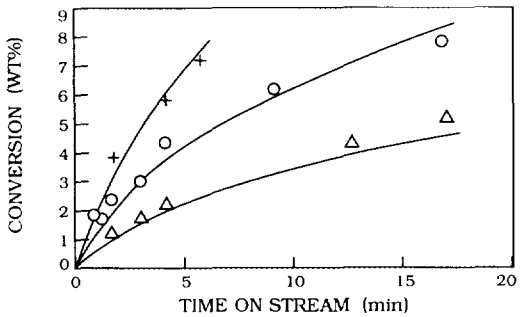


FIG. 6. Theoretical curves and experimental points for the reaction of 2-methylpentane on USHY at 300°C, catalyst-to-reactant ratios: (△) 0.0077, (○) 0.0166, and (+) 0.0229.

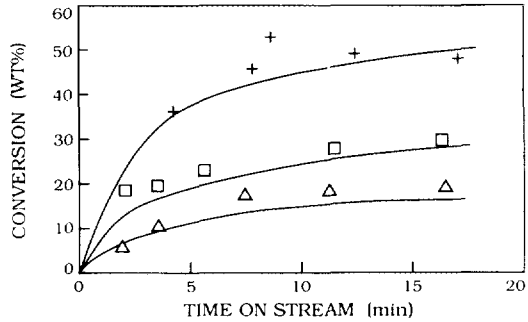


FIG. 8. Theoretical curves and experimental points for the reaction of 2-methylpentane on USHY at 450°C, catalyst-to-reactant ratios: (△) 0.0077, (□) 0.0229, and (+) 0.106.

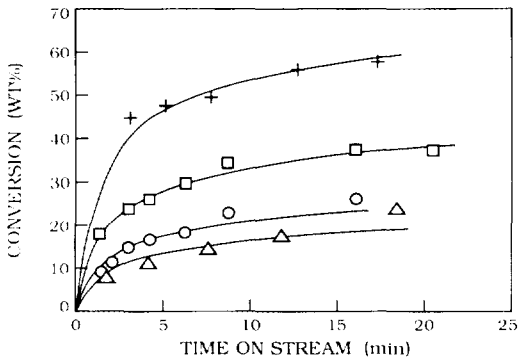


FIG. 9. Theoretical curves and experimental points for the reaction of 2-methylpentane on USHY at 500°C, catalyst-to-reactant ratios: (△) 0.0079, (○) 0.013, (□) 0.035, and (+) 0.108.

that chain cracking and/or adsorption phenomena are significantly different for the linear and branched paraffins. We can suspect that branched paraffins in general, and 2-methylpentane in particular, have a larger proportion of conversion proceeding via the chain process.

Parameter B reflects the relative value of the adsorption constants of the reactant and products as described in Eq. (12c). Its value was found to become more negative with increasing reaction temperature, changing from −0.901 at 300°C to −0.999 at 500°C. Examination of Eq. (12c) indicates that this constitutes evidence that products are more strongly adsorbed on the active sites, relative to feed molecules, at all our experimental conditions and that this trend increases with temperature. Similar behaviour in the change of $B$ with temperature was reported by Abbot and Wojciechowski, who studied $n$-hexadecane (*21*) and 2,2,4 trimethylpentane (*11*) reactions in a HY zeolite in the temperature range 300 to 400°C but is opposite to the trend reported in $n$-nonane cracking (*1*), indicating that the competition for adsorption sites is closely related to feed and/or product properties and perhaps to subtle changes in catalyst composition.

TABLE 4

Optimum Values for Kinetic Parameters for Cracking of 2-Methylpentane at Various Temperatures ($N$ fixed at 1.0)

| Kinetic parameters | Temperature (°C) | | | |
|---|---|---|---|---|
| | 300 | 400 | 450 | 500 |
| $A_1$ (min$^{-1}$) | 0.0786 | 0.355 | 0.540 | 1.015 |
| $A_2$ (min$^{-1}$) | −0.0085 | −0.031 | −0.146 | −0.152 |
| $B$ | −0.901 | −0.960 | −0.996 | −0.999 |
| $G$ (min$^{-1}$) | 0.118 | 0.251 | 0.231 | 0.301 |
| $N$ | 1.0 | 1.0 | 1.0 | 1.0 |
| $\Sigma\, \mathcal{F}_i$ | 1.050 | 1.270 | 1.470 | 1.760 |
| $C_{A_0}$ (mol dm$^{-3}$) | 0.021 | 0.018 | 0.017 | 0.016 |

Examination of Eq. (12c) reveals that the large negative values for $B$ require that both

$$\Sigma K_{P_i}\, \mathcal{F}_i\, C_{A_0} \gg 1 \qquad (16)$$

and

$$\Sigma K_{P_i}\, \mathcal{F}_i \gg K_A. \qquad (17)$$

Equation (12c) therefore reduces to

$$B = \frac{K_A}{\Sigma K_{P_i}\, \mathcal{F}_i} - 1 \qquad (18)$$

and

$$B + 1 = \frac{K_A}{\Sigma K_{P_i}\, \mathcal{F}_i} = \frac{K_A}{\bar{K}_P \Sigma\, \mathcal{F}_i} \qquad (19)$$

where $\bar{K}_P = \Sigma K_{P_i}\, \mathcal{F}_i / \Sigma\, \mathcal{F}_i$ is the weighted average adsorption constant for product species. $\Sigma\, \mathcal{F}_i$ can be calculated from the sum of the molar selectivities of initial products and is given in Table 4. Rearranging Eq. (19) we get

$$\frac{K_A}{\bar{K}_P} = (B + 1)\, \Sigma\, \mathcal{F}_i. \qquad (20)$$

Using Eq. (20), values representative of the ratio of the adsorption constants have been calculated and are listed in Table 5. From these, a plot of log ($K_A/K_P$) vs $1/T$ has been generated and is shown in Fig. 10. The value for the difference in enthalpy of adsorption between feed and the average product, $\Delta\Delta H_{Ads.}$, is estimated at 73 kJ/mol for the 300–500°C temperature range. This difference in the enthalpy of adsorption together with the large negative value of B at all temperatures indicates that both here

TABLE 5

Values of Various Derived Constants for Cracking of 2-Methylpentane at Various Temperatures

| | Temperature (°C) | | | |
|---|---|---|---|---|
| | 300 | 400 | 450 | 500 |
| (1) $\frac{K_A}{\bar{K}_P}$ | 0.104 | 0.051 | 0.006 | 0.002 |
| $A_1$ (min$^{-1}$) | 0.0786 | 0.355 | 0.540 | 1.015 |
| (2) $A_1 + A_2$ (min$^{-1}$) | 0.0701 | 0.324 | 0.394 | 0.863 |
| (3) $A_2$ (min$^{-1}$) | −0.0085 | −0.031 | −0.146 | −0.152 |
| (4) $\Sigma k_{M_i}[S_0]$ (mol dm$^{-3}$ min$^{-1}$) | 0.015 | 0.1466 | 1.659 | 13.596 |

*Note.* (1) Determined according to Eq. (9); (2) monomolecular rate constant; (3) bimolecular rate constant; (4) determined according to Eq. (11).

and in *n*-nonane cracking the surface is mostly covered by the carbenium ions of product olefins and that $\bar{K}_P \gg K_A$. However, in 2-methylpentane, the enthalpy of adsorption is higher for the reactants, while the opposite is true for *n*-nonane (*1*). Since the product olefins are similar in both cases, and presumably form carbenium ions exothermally, we are lead to the conclusion that the process of carbonium ion formation is exothermic for 2-methylpentane and endothermic for *n*-nonane. We will be better able to comment on this issue when we examine product selectivities and reaction path probabilities for the two cases.

From Fig. 11 it can be seen that the value of $A_1$ increases with temperature, confirming that catalyst activity increases with reaction temperature. This is supported qualitatively by the shape and position of the conversion vs time-on-stream plots presented in Figs. 6 to 9.

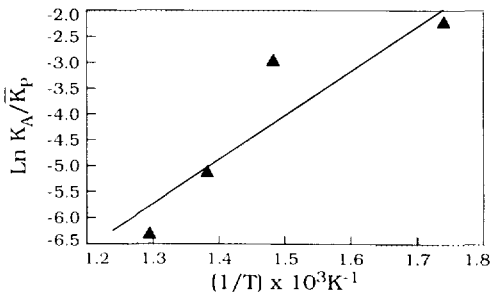


FIG. 10. Variation of the ratio $K_A/\bar{K}_P$ with reaction temperature.

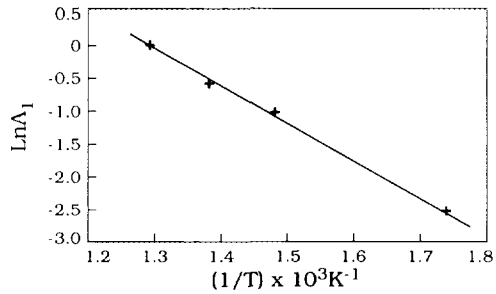


FIG. 11. Variation of $A_1$ with reaction temperature.

Further information about the reaction rate constants can be extracted from the results presented in Table 4 by using Eqs. (12a), (12b), and (18). Adding Eqs. (12a) and (12b), we obtain a measure of the rate of monomolecular cracking:

$$A_1 + A_2 = \frac{\Sigma k_{M_i} K_A}{1 + \Sigma K_{P_i} \mathcal{F}_i C_{A_0}} [S_0]. \quad (21)$$

Remembering the high surface coverage approximation described by Eq. (16) and substituting (16) and (19) into (21), we extract the total specific rate of monomolecular cracking:

$$\Sigma k_{M_i} [S_0] = C_{A_0} \frac{A_1 + A_2}{B + 1}. \quad (22)$$

Using Eq. (22) the values of $\Sigma k_{M_i} [S_0]$ have been calculated for the four temperatures and are listed in Table 5. In Fig. 12, these values reveal that the rate constant for monomolecular reactions increases nonlinearly with increasing reaction temperature. This finding is consistent with product distribution data which shows that the relative importance of the various cracking modes changes with temperature (*36*). At low temperatures, cracking involving C–C scission at various positions in the molecule dominates, while contributions from initiation by hydride abstraction to form $H_2$ and a trend of center bond cracking to produce more $C_3$ species dominate at

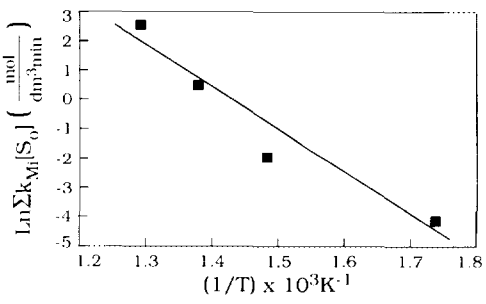


FIG. 12. Arrhenius plot for 2-methylpentane protolysis on USHY.

high temperatures. Presumably these processes emerge at higher temperatures because they require higher activation energies and the contribution of their rate constants leads to the concavity of the Arrhenius plot in Fig. 12.

Using the values of $\Sigma k_{M_i}[S_0]$ from Table 5 and correlating with a straight line leads to a value of 121 kJ/mol for the average activation energy for 2-methylpentane cracking over USHY in the 300–500°C temperature range. This value is of the same order of magnitude as that reported for *n*-hexane cracking (126–143 kJ/mol) over aluminosilicate catalysts in the temperature range 320–450°C (*21*, *37*). It is not reported if these latter catalysts were operating in the monomolecular or the bimolecular regime as the kinetic model used did not account for such subtleties. The value is also in keeping with an exothermic enthalpy of adsorption since the activation energy of 121 kJ/mol is quite a bit higher than the endothermicity of forming the observed products from 2-methylpentane cracking. This confirms our conclusion that for some reason carbonium ion formation is exothermic for 2-methylpentane and endormic for *n*-nonane (*1*) and cumene (*38*). The difference may well be due to subtle differences in catalyst steaming and calcination rather than depending on reactant properties alone.

In Eq. (12b), the term $\Sigma k_{C_i} K_{P_i} \mathcal{F}_i$ contains the chain reaction rate constants, adsorption constants for products, and the total moles of each product formed. Since all these terms change with temperature, a value for the sum of chain reaction rate constants ($\Sigma k_{C_i}$) cannot be readily extracted from our results.

*Activity decay.* It can be seen from Table 4 that the deactivation rate constant $G$ increases with temperature, showing that in 2-methylpentane cracking on USHY, the catalyst decays faster at higher reaction temperatures. The effect is seen qualitatively in the more rapid flattening of the conversion curves in Fig. 9 compared to Fig. 6 and is attributable in part to a change in the contribution made by chain processes, which dominate at lower reaction temperatures. The chain processes offer a route by which surface species, which can undergo undesirable "coking" reactions, are cleared from the catalyst surface. This is accomplished by the hydrogenation of surface carbenium ions by feed molecules and can forestall the formation of poisonous dehydrogenated species. Since the role played by chain reactions (disproportionations) decreases with reaction temperature, while at the same time the $B$ parameter indicates more successful competition for adsorption on active sites by carbenium ions, the ability of the catalyst surface to shed potential poison precursors is reduced at higher temperatures. Such behaviour is in direct contrast to the decay behaviour in *n*-nonane cracking.

It is interesting to note that the value of the deactivation rate constant for *n*-hexane cracking ($G$ = 0.88 min.$^{-1}$) on USHY at 500°C (*22*) is higher by a factor of three than that for 2-methylpentane ($G$ = 0.30 min.$^{-1}$). A plausible explanation for this difference is that 2-methylpentane, having a tertiary hydrogen, will more readily donate hydride ions and promote chain reactions which regenerate active sites and prevent decay. Such an explanation is supported by the observation that the kinetics of *n*-hexane cracking are adequately described using the monomolecular model with $A_2 = 0$. Note also that olefins, which are hydrogen poor to start with, are notorious for causing the rapid decay of catalysts. For example, the values of the deactivation rate constants for

1-octene (*39*) and 1-hexene (*39*) cracking over USHY at 300°C are 37 and 60 $min^{-1}$, respectively, more than two orders of magnitude greater than that for 2-methylpentane at 500°C. Presumably this arises because a hydrogen transfer reaction from a feed olefin molecule to a carbenium ion results in the formation of an unsaturated, olefinic carbenium ion whose chances of desorption are less than those of a paraffinic carbenium ion. Interestingly, the longer chain 1-octene has a lower decay constant, perhaps because it can donate a hydrogen more readily than 1-hexene. This suggests that the decay rate for large olefin cracking should approach that of the corresponding paraffin.

## CONCLUSIONS

We propose that all cracking reactions proceed via chain processes to some extent. The initiation of the cracking reaction and the formation of the initial carbenium ion is due to the protonation of a double bond in the case of olefin cracking and by protolysis in the case of paraffins. Termination of the chain is by the desorption of a carbenium ion as an olefin. Between initiation and termination, chain reactions are propagated by reactions between gas-phase molecules and surface carbenium ions. If hydrogen transfer takes place from a feed molecule the original carbenium ion is replaced by the carbenium ion of the feed molecule. This can crack or isomerize before either desorbing as an olefin or undergoing a subsequent hydrogen transfer reaction. If an isomerized parent carbenium ion undergoes hydrogen transfer, the product is an isomer of the feed molecule. This mechanism explains the formation of isomers of paraffinic feed molecules without invoking the concept of carbonium ion isomerization.

Our mechanism also explains the enrichment of the product in paraffins which occurs whenever a propagation reaction with a surface carbenium ions takes place. In principle, each initiation produces one molecule of paraffin product. So does each chain event. Thus, the total selectivity for product paraffins must be equal to at least one. Higher total paraffin selectivities arise when hydrogen is transferred from coke to saturate product olefins and form "excess" paraffins, but in no case can the sum of paraffin selectivities be less than one. On the other hand, the sum of olefin selectivities can be greater or less than one since olefins appear in all termination reactions and by $\beta$-cracking but no olefins are formed in the chain processes. If the gas-phase molecule giving up the hydride in a chain event is a product olefin, this process will lead to the formation of "excess" paraffin and an olefin carbenium ion $C_nH_{2n-1}^+$ which represents a species on its way to form coke and poison a site.

Finally, the contribution of chain processes to the overall reaction governs the size of the $A_2$ parameter. From Eq. (15) and the definition of $A_2$ given in Eq. (12b) we see that long chains are encouraged by:

1. a high selectivity for olefins (high $\alpha_n$)
2. strong adsorption of carbenium ions (high ${}_nK_n$)
3. high reactivities of surface carbenium ions toward bimolecular reactions (high $I_n$)
4. low reactivity of Brønsted sites for protolysis (low $I_1$)
5. low coverage by carbonium ions (low $k_0/k_{-0}$)
6. high reactant partial pressures (high $[C_6H_{14}]_0$)
7. high concentration of product (or added) olefins (high $X$).

Although all of these factors can be used to alter catalyst performance, the most common distortions in cracking catalyst evaluation are due to the presence of impurities, diluents, additives, or carrier gases in various catalytic cracking studies. These will clearly change $[C_6H_{14}]_0$ as well as the parameters defined by Eq. (12) and hence both the kinetics and product selectivity. All such diluents and additives change the kinetic chain length by displacing carbenium ions off the surface. Some may also take part in chain propagation. Even nitro-

gen has an effect on the chain length and hence on the selectivity and activity.

We have shown that our model, based on initiation by monomolecular protolytic cracking followed by a bimolecular chain mechanism involving surface carbenium ions and using the time on stream theory of catalyst decay, fits the data for the conversion of 2-methylpentane on USHY zeolite in the temperature range 300–500°C. Interpretation of the parameters obtained from the model provides a cohesive picture of changes in the reaction mechanism with increase in reaction temperature.

The model shows that product species are more strongly adsorbed on active sites than the feed and that competitive inhibition caused by the occupation of sites by product species increases with increasing reaction temperature. At the same time, the rate of catalyst decay increases slowly with increasing reaction temperature mainly, we believe, because at high temperatures chain reactions, responsible for hydrogen transfer, are less important and surface carbenium ions can more readily progress to "coke."

Clearly the adsorption and reaction parameters are very different for 2-methylpentane than for *n*-paraffins (*1*). However, the same types of chemical processes take place in all cases, only the rate parameters and their relative sizes differ between molecules or molecular classes. The model and the interpretation methods described here should be applicable to a wide range of cracking reactions involving olefins and paraffins, both branched and linear, as well as to cycloparaffins and other, more exotic, molecular configurations. Such a generalized model holds promise of yielding comparable kinetic parameters whose values will lead to a better understanding of the influence of catalyst properties on cracking rates and mechanisms.

## APPENDIX A

### *Part I*

To obtain the rate expression, we assume

1. The skeletal isomerization of carbenium ions is at equilibrium. That is,

$$\frac{[i\text{-}C_nH_{2n+1}S^+]}{[C_nH_{2n+1}S^+]} = \frac{{}_nk_{in}}{{}_{in}k_n} = K_{nn} \quad n > 4. \tag{I-1}$$

2. The concentration of $C_6H_{15}S^+$ ion is negligible relative to that of reactant or product and its rate of change is negligible compared with that of reactant. Then the steady-state approximation may be used and gives

$$[C_6H_{15}S^+] = \frac{k_0}{I_0}[C_6H_{14}][SH], \tag{I-2}$$

where $I_0 = \Sigma_0 k_{in} + k_{-0}$.

3. From our experimental data (Table 1) we note that there is no product with carbon number $\geq 7$ in the initial product distribution. We may take it that the concentration of these larger carbenium ions is 0.

$$[C_nH_{2n+1}S^+] = 0 \quad \text{for } n \geq 7. \tag{I-3}$$

Applying the above assumptions to the chain mechanism consisting of Eqs. (6)–(10), the rate of formation of individual product paraffins and hydrogen may be written in matrix form,

$$\begin{vmatrix} r_{H_2} \\ r_{CH_4} \\ r_{C_2H_6} \\ r_{C_3H_8} \\ r_{C_4H_{10}} \\ r_{C_5H_{12}} \\ r_{C_6H_{14}} \end{vmatrix} = \begin{vmatrix} {}_0k_{16} & 0 & 0 & 0 & 0 & 0 \\ {}_0k_{15} & {}_2k_{27} & {}_3k_{28} & {}_4k_{29} & {}_5k_{210} & {}_6k_{211} \\ {}_0k_{14} & {}_2k_{26} & {}_3k_{27} & {}_4k_{28} & {}_5k_{29} & {}_6k_{210} \\ {}_0k_{13} & {}_2k_{25} & {}_3k_{26} & {}_4k_{27} & {}_5k_{28} & {}_6k_{29} \\ {}_0k_{12} & {}_2k_{24} & {}_3k_{25} & {}_4k^*_{26} & {}_5k_{27} & {}_6k_{28} \\ 0 & {}_2k_{23} & {}_3k_{24} & {}_4k_{25} & {}_5k^*_{26} & {}_6k_{27} \\ 0 & 0 & 0 & 0 & 0 & {}_6k^*_{26} \end{vmatrix} \begin{vmatrix} k_0[SH]/I_0 \\ [C_2H_5S^-] \\ [C_3H_7S^-] \\ [C_4H_9S^+] \\ [C_5H_{11}S^-] \\ [C_6H_{13}S^-] \end{vmatrix} [C_6H_{14}], \tag{I-4}$$

where

$$ {}_4k_{26}^{*} = {}_4k_{26} + {}_{i4}k_{26}K_{44} $$

$$ {}_5k_{26}^{*} = {}_5k_{26} + {}_{ik}k_{26}K_{55} $$

$$ {}_6k_{26}^{*} = {}_{i6}k_{26}K_{66} $$

and the overall rate may be written

$$ -r_{\text{overall}} = [I_1\ I_2\ I_3\ I_4\ I_5\ I_6] \begin{vmatrix} k_0[\text{SH}]/I_0 \\ [C_2H_5S^+] \\ [C_3H_7S^+] \\ [C_4H_9S^+] \\ [C_5H_{11}S^+] \\ [C_6H_{13}S^+] \end{vmatrix} [C_6H_{14}], \qquad \text{(I-5)} $$

where

$$ I_1 = \sum_{n=2}^{6} {}_0k_{1n} $$

$$ I_2 = \sum_{j=3}^{7} {}_2k_{2j} $$

$$ I_3 = \sum_{j=4}^{8} {}_3k_{2j} $$

$$ I_4 = \sum_{j=5}^{9} {}_4k_{2j} + {}_{i4}k_{26}\,K_{44} $$

$$ I_5 = \sum_{j=6}^{10} {}_5k_{2j} + {}_{i5}k_{26}\,K_{55} $$

$$ I_6 = \sum_{j=7}^{11} {}_6k_{2j} + {}_{i5}k_{26}\,K_{66}. $$

From Eqs. (I-4) and (I-5),

$$ -r_{\text{overall}} = r_{H_2} + r_{CH_4} + r_{C_2H_6} + r_{C_3H_8} + r_{C_4H_{10}} + r_{C_5H_{12}} + r_{iC_6H_{14}}. \qquad \text{(I-6)} $$

To obtain the concentrations of carbenium ions, values which cannot be determined by experiment, we assume that the adsorption of product olefins reaches equilibrium. From Eq. (10), we have

$$ \begin{vmatrix} [C_2H_5S^+] \\ [C_3H_7S^+] \\ [C_4H_9S^+] \\ [C_5H_{11}S^+] \\ [C_6H_{13}S^+] \end{vmatrix} = \begin{vmatrix} {}_2K_2 & 0 & 0 & 0 & 0 \\ 0 & {}_3K_3 & 0 & 0 & 0 \\ 0 & 0 & {}_4K_4 & 0 & 0 \\ 0 & 0 & 0 & {}_5K_5 & 0 \\ 0 & 0 & 0 & 0 & {}_6K_6 \end{vmatrix} \begin{vmatrix} [C_2H_4] \\ [C_3H_6] \\ [C_4H_8] \\ [C_5H_{10}] \\ [C_6H_{12}] \end{vmatrix} [\text{SH}], \qquad \text{(I-7)} $$

where ${}_nK_n = {}_0k_n/{}_nk_0 = [C_nH_{2n+1}S]^+/[C_nH_{2n}][\text{SH}]$ is the adsorption constant of olefin $C_nH_{2n}$.

Now, an active site balance is carried out using the expression

$$ [\text{SH}] = [\text{SH}](1 + Gt)^{-N} - \left([C_6H_{15}S^+] + \sum_{n=2}^{6} [C_nH_{2n+1}S^+] + \sum_{n=4}^{6} [iC_nH_{2n+1}S^+]\right). \qquad \text{(I-8)} $$

Substituting Eqs. (I-1), (I-2), and (I-7) into Eq. (I-8) and rearranging gives

$$ [\text{SH}] = \frac{(1 + Gt)^{-N}[\text{SH}]_0}{1 + k_0[C_6H_{14}]/I_0 + \Sigma_{n=2}^{6}\ {}_nK_n[C_nH_{2n}] + \Sigma_{n=4}^{6}\ {}_nK_n\,K_{nn}[C_nH_{2n}]}. \qquad \text{(I-9)} $$

For all primary products, it is assumed that the concentration of product is proportional to the conversion of reactant, i.e.,

$$[C_nH_{2n}] = \mathcal{F}_n([C_6H_{14}]_0 - [C_6H_{14}]). \quad \text{(I-10)}$$

Expressing the concentration of reactant in terms of fractional conversion $X$,

$$[C_6H_{14}] = [C_6H_{14}]_0 \left(\frac{1 - X}{1 + \varepsilon X}\right). \quad \text{(I-11)}$$

Substituting Eq. (I-11) into Eq. (I-10) gives

$$[C_nH_{2n}] = \mathcal{F}_n \left(1 - \frac{1 - X}{1 + \varepsilon X}\right) [C_6H_{14}]_0 \quad \text{(I-12)}$$

$$[C_nH_{2n}] = b_n \frac{X}{1 + \varepsilon X} [C_6H_{14}]_0, \quad \text{(I-13)}$$

where $\mathcal{F}_n$ is the corrected molar selectivity of olefin $C_nH_{2n}$. $b_n$ is the experimental molar selectivity of olefin $C_nH_{2n}$
and

$$\mathcal{F}_n = b_n/(1 + \varepsilon). \quad \text{(I-14)}$$

For a plug flow reactor, we have

$$r_{\text{overall}} = \frac{dX}{d\tau} [C_6H_{14}]_0. \quad \text{(I-15)}$$

Finally, from Eqs. (I-5), (I-7), (I-9), (I-11), (I-12), and (I-15) we obtain the rate expression for overall reaction as given in Eq. (11a).

Integrating Eq. (11a) gives Eq. (11b). The integration constants $\phi_i$ have the forms:

$$\phi_1 = (1 + \epsilon)/A_1 - (2\epsilon - B)(\epsilon + 1_1)/(A_1\epsilon - A_2) + \epsilon(\epsilon - B)(\epsilon + 1)A_1/(A_1\epsilon - A_2)^2$$

$$\phi_2 = A_1 + A_2$$

$$\phi_3 = A_1\epsilon + A_2$$

$$\phi_4 = (1 + \epsilon)/A_1$$

$$\phi_5 = \epsilon(\epsilon - B)/A_1\epsilon - A_2$$

$$\phi_6 = g_1 L_n(A_1 + A_2).$$

*Part II*

According to the definition of KCL (Eq. (14)), we have

$$\text{KCL} = \frac{k_0 \sum_{n=2}^{6} {}_0k_{1n} [C_6H_{14}][SH]/I_0 + \sum_{n=2}^{6} I_n[C_nH_{2n+1}S^+][C_6H_{14}]}{k_0 \sum_{n=2}^{6} {}_0k_{1n} [C_nH_{14}][SH]/I_0}. \quad \text{(II-1)}$$

Substituting Eqs. (I-7), (I-12) into Eq. (II-1), and comparing with Eq. (12), gives Eq. (15).

## APPENDIX B: NOMENCLATURE

| | |
|---|---|
| $r$ | = the net rate of surface species concentration change |
| $[P_iS]$ | = concentration of the $i$th surface ion |
| $[P_i]$ | = concentration of the $i$th product species |
| $[S_0]$ | = concentration of active sites (initial) |
| $G$ | = aging parameter ($\text{min}^{-1}$) (function of temperature) |
| $M$ | = aging exponent dimensionless |
| $t$ | = catalyst time on stream during an experimental run (min) |
| $C_6H_{14}$ | = a feed molecule, 2-methylpentane |
| SH | = a Brønsted acid site |
| $C_nH_{2n+1}S^+$, $C_jH_{2j+1}S^+$ | = a carbenium ion associated with a Brønsted site |
| $i$-$C_nH_{2n+1}S^+$ | = a skeletal isomer of $C_nH_{2n+1}S^+$ ion |
| $C_{6-n}H_{2(6-n)+2}$ | = a product paraffin (including hydrogen) from chain initiation |
| $C_{6+n-j}H_{2(6+n-j)+2}$ | = a product paraffin from chain propagation |
| $C_{j-n}H_{2(j-n)}$ | = a product olefin from $C_jH_{2j+1}S^+$ ion $\beta$-cracking |

$C_nH_{2n}$ = a product olefin from chain temperature (desorption)
$X$ = instantaneous fractional conversion of feed at time $t$ (dimensionless)
$\tau$ = space time (min)
$\varepsilon$ = volume expansion
$N$ = aging exponent
$A_1$, $A_2$, $B$ = kinetic parameters
$\mathcal{F}_n$ = molar selectivity of product olefin $C_nH_{2n}$
$[C_6H_{14}]_0$ or $C_{A_0}$ = concentration of feed (initial)
$K_A$ = adsorption constant of feed molecule
$K_{nn}$ = skeletal isomerization constant for $C_nH_{2n+1}S^+$ ion (function of temperature)
$K_{P_i}$ or ${}_nK_n$ = adsorption constant of the $i$th product olefin ($C_nH_{2n}$)
$K_P$ = average adsorption constant for the products.
$\rho$ catalyst-to-reactant weight ratio
$b$ = reactant to catalyst density ratio
$t_f$ = total run time of the experiment (min)
$\phi_i$ = a function of kinetic parameters $A_1$, $A_2$, $B$, $G$
KCL = an instantaneous kinetic chain length (dimensionless)
$X_f$ = instantaneous fraction conversion at time $t_f$
$\tau_f$ = space time at time $t_f$ (min)
$\overline{X}_f$ = average fractional conversion (dimensionless)
$-r_{\text{overall}}$ = overall rate
$k$ = rate constant of an elementary reaction
$k_{M_i}$ or ${}_0k_{1_i}$ = is the rate constant for $i$th mode of monomolecular reaction. (initiation)
$\Sigma_j k_{C_i}$ = is the sum of the rate constants for the $j$-modes of bimolecular reaction between product $i$ and the reactant molecule.
$I_n$ = a function of rate constants

## REFERENCES


1. Groten, W. A., and Wojciechowski, B. W., submitted for publication.
2. Anufrief, D. M., Kuznetsov, P. N., and Lone, K. G., *J. Catal.* **65,** 221 (1980).
3. Haag, W. D., and Dessau, R. M., *in* "Proceedings, 8th International Congress on Catalysis, Berlin, 1984," Vol. II, p. 305. Dechema, Frankfurt-am-main, 1984.
4. Corma, A., Planelles, J., Sanchez, J., and Tomas, F., *J. Catal.* **92,** 284 (1985).
5. Kramer, G. M., McVicker, G. B., and Ziemiak, J. J., *J. Catal.* **92,** 355 (1985).
6. Corma, A., Planelles, J., Sanchez, J., and Thomas, F., *J. Catal.* **93,** 30 (1985).
7. Corma, A., Planelles, J., and Thomas, F., *J. Catal.* **94,** 445 (1985).
8. Lombardo, E. A., Pierantozzi, R., and Hall, W. K., *J. Catal.* **110,** 171 (1988).
9. Lombardo, E. A., and Hall, W. K., *J. Catal.* **112,** 565 (1988).
10. Abbot, J., and Wojciechowski, B. W., *Can. J. Chem. Eng.* **66,** 825 (1988).
11. Abbot, J., and Wojciechowski, B. W., *J. Catal.* **113,** 353 (1988).
12. Abbot, J., and Wojciechowski, B. W., *J. Catal.* **115,** 1 (1989).
13. Hall, W. K., Lombardo, E. A., and Engelhardt, J., *J. Catal.* **115,** 611 (1989).
14. Kramer, G. M., and McVicker, G. B., *J. Catal.* **115,** 608 (1989).
15. Hattori, H., Takahaski, O., Tagaki, M., and Tanabe, K., *J. Catal.* **68,** 132 (1981).
16. Shih, S., *J. Catal.* **79,** 390 (1983).
17. Weisz, P. B., *Annu. Rev. Phys. Chem.* **21,** 175 (1970).
18. Pickert, P. E., Rabo, J. A., Dempsey, E., and Schomaker, V., "Proceedings, 3rd International Congress on Catalysis, Amsterdam, 1964," Vol. II, p. 1264. North-Holland, Amsterdam, 1965.
19. Tung, S. E., and McInnch, E., *J. Catal.* **10,** 166 (1968).

20. Abbot, J., and Wojciechowski, B. W., *J. Catal.* **104,** 80 (1987).
21. Abbot, J., and Wojciechowski, B. W., *J. Catal.* **109,** 274 (1988).
22. Abbot, J., and Wojciechowski, B. W., *Can. J. Chem. Eng.* **66,** 825 (1988).
23. Ko, A. N., and Wojciechowski, B. W., *Prog. React. Kinet.* **12**(4), 201 (1983).
24. Wojciechowski, B. W. *Catal. Rev. Sci. Eng.* **9**(1), 79 (1974).
25. Wojciechowski, B. W., *Can. J. Chem. Eng.* **46,** 48 (1968).
26. Groten, W. A., and Wojciechowski, B. W., *J. Catal.* **122,** 362 (1990).
27. Abbot, J., and Wojciechowski, B. W., *J. Catal.* **107,** 451 (1987).
28. Krzywicki, A., and Marczewski, M., *J. Chem. Soc. Faraday Trans.* **76,** 1311 (1980).
29. Daage, M., and Fajula, F., *J. Catal.* **81,** 394 (1983).
30. Daage, M., and Fajula, F., *J. Catal.* **81,** 100 (1983).
31. Rice, N. M., and Wojciechowski, B. W., *Can. J. Chem. Eng.* **69,** 1100 (1991).
32. Pansing, W. F., *J. Phys. Chem.* **69,** 392 (1965).
33. Weisz, P., *Chem. Tech.*, 498 (1973).
34. Corma, A., Monton, J. B., and Orchilles, A. V., *Appl. Catal.* **16,** 59 (1985).
35. Maganotta, V. L., and Gates, B. C., *J. Catal.* **46,** 266 (1977).
36. Bamwenda, G. R., and Wojciechowski, B. W., submitted for publication.
37. Miale, J. N., Chen, N. Y. and Weisz, *J. Catal.* **6,** 287 (1966).
38. Best, D. A., and Wojciechowski, B. W., *J. Catal.* **47,** 343 (1977).
39. Abbot, J., and Wojciechowski, B. W., *J. Catal.* **108,** 346 (1987).